BISMUTH OXIDE AS AN ADDITIVE IN PASTED ZINC ELECTRODES*

J. McBREEN and E. GANNON

Department of Applied Science, Brookhaven National Laboratory, Upton, NY 11973 (U.S.A.)

(Received January 2, 1985; in revised form April 19, 1985)

Summary

The effect of small additions (2 - 10 wt.%) of Bi_2O_3 to zinc electrodes has been studied using chronopotentiometry, cyclic voltammetry, and polarization studies. Methods were devised for preparing electrode samples for scanning electron microscopy so that the bismuth deposits could be clearly observed. In addition, studies were carried out into zinc deposition on bismuth single-crystals in zincate electrolytes, in an effort to elucidate the interaction of zinc with bismuth. Investigations were also carried out on silver electrodes in bismuth oxide-saturated zincate electrolytes. The chronopotentiometry results indicate that the Bi_2O_3 additive is essentially quantitatively reduced to bismuth prior to deposition of zinc. The reduced Bi_2O_3 forms a bismuth matrix in the electrode and consists of needle-like deposits. The nucleation overvoltage for zinc deposition on bismuth is ≈ 20 mV. The deposits have an hexagonal morphology. The beneficial effect of bismuth appears to accrue from the conductive bismuth matrix and the maintenance of an active deposit.

Introduction

There have been several reports on the beneficial effect of bismuth oxide additives in zinc electrodes [1 - 3]. However, the precise mechanism by which the bismuth oxide enhances capacity maintenance on cycling was not established.

The present study was very similar to previous work carried out on several other metal oxide additives in zinc electrodes [4]. In this investigation, the deposition of bismuth during the formation cycle was studied using chronopotentiometry, cyclic voltammetry, and scanning electron microscopy. In addition, the deposition of zinc from zincate electrolytes on single-crystal bismuth was investigated. Studies were also conducted into

*This research was performed under the auspices of the U.S. Department of Energy under Contract No. DE-AC02-76CH00016.

Elsevier Sequoia/Printed in The Netherlands

zinc deposition on silver in bismuth oxide-saturated zincate electrolytes. The deposition studies on bismuth and silver were done in an attempt to understand the interaction of zinc with the silver current-collector and the bismuth formed in the zinc electrode. The techniques used were the potential-step method, cyclic voltammetry, and X-ray diffraction.

Experimental

Bi_2O_3 in pasted zinc electrodes

Cell

All electrochemical measurements on pasted zinc electrodes were carried out in 2 A h zinc/nickel oxide cells. Details of the electrode preparation and cell construction have been given previously [4]. The specifications of the zinc electrodes are given in Table 1.

TABLE 1

Specifications of the zinc electrode

ZnO content	7.20 g
PTFE content	0.15 g
Electrode dimensions	7.62 × 5.08 × 0.07 cm
Current collector	Expanded silver (Exmet Corp. 5 Ag 12.5-2/o)

Experimental procedure

After cell assembly, the cells were vacuum treated and backfilled with nitrogen. Prior to filling the cells, the electrolyte (8.4M KOH + 0.5M LiOH + 0.74M ZnO) was de-aerated by sparging with nitrogen. After the cells were filled, the cell ports were sealed and the cells were soaked for 24 h prior to the start of electrochemical measurements.

In the case of the chronopotentiometry measurements, the cells were charged at 150 mA (3.87 mA cm^{-2}) and the zinc electrode potential was monitored for the first two hours of charge.

Cyclic voltammetry was carried out in some cells. The sweep rate was 50 mV s^{-1}. The positive limit of the voltage envelope was 0.0 V. the negative limit was varied in various increments from −0.2 to −1.5 V. Note, all potentials reported in this paper are with respect to the Hg/HgO electrode in the same electrolyte, unless otherwise specified.

The other electrochemical measurement was a determination of the zinc electrode polarizability. For this test, the cell was charged at 150 mA for 17 h, discharged at 500 mA for 2 h, and recharged at 200 mA for 5 h. After standing in the charged state for 17 h, the zinc electrode polarizability was determined by carrying out cyclic voltammetry at 1 mV s^{-1} - 10 mV s^{-1} in a narrow voltage envelope about the reversible potential of the zinc electrode.

Electron microscopy

After completion of the formation charge, the zinc electrodes were washed repeatedly in distilled water, rinsed successively with methanol and acetone, and then dried under nitrogen. The dried electrodes were soaked in a 10M NH_4OH + 1M NH_4Cl solution at 20 °C for 6 h to remove the zinc oxide. The electrode was washed repeatedly with water, rinsed successively with 0.5M perchloric acid, methanol and acetone, and dried again under nitrogen prior to the electron microscopy study. Without the perchloric acid rinse, the electron micrographs were of poor quality. This apparently was due to the tendency of bismuth to form oxy-salts, that adhere to the bismuth surface. The perchlorate does not form an oxy-salt and subsequent rinses yield a clean bismuth surface.

Deposition of zinc on bismuth

Electrode preparation

For the electron microscopy and X-ray studies, bismuth electrodes were prepared by melting (in a small glass beaker, dia. = 2 cm) 10 g of polycrystalline bismuth in a tube furnace at 300 °C. The furnace was shut off and allowed to cool overnight. The process invariably yielded single crystals of bismuth. A copper wire lead was soldered on to the back of the electrode. The lead and the back of the electrode were masked with epoxy. The front of the electrode was successively polished with 400 grit and 600 grit sandpaper. Prior to the electrochemical experiments, the electrodes were electropolished in aqueous, saturated KI solution containing 20 ml l^{-1} of concentrated HCl [5]. During the electropolishing process, the electrode was anodized at 20 mA cm^{-2} for four, 30 s periods with 5 min rest periods in between. The electrodes were then rinsed repeatedly with triply-distilled water prior to incorporation into the cell. The electrodes for the cyclic-voltammetry and potential-step measurements were prepared in a similar fashion. These electrodes were cylindrical (dia.: 0.75 cm, length: 1.5 cm).

Electron microscopy and X-ray studies

Sample preparation for the scanning electron microscopy and X-ray diffraction studies was as follows. Zinc was deposited on the bismuth electrode at 15 mA cm^{-2} in 8.4M KOH + 0.74M ZnO. The electrode was immediately removed from the electrolyte, washed repeatedly in distilled water, rinsed in acetone, and dried over nitrogen. The electrode was stored under nitrogen until mounted in either the scanning electron microscope or the X-ray goniometer.

Cyclic voltammetry and potential step measurements

Details of the cell and the procedures for conducting these measurements are given elsewhere [6].

Deposition of zinc on silver

Investigations were carried out into the electrodeposition of zinc on silver in bismuth oxide-saturated zincate electrolyte. The electrolyte was pre-

pared by adding excess Bi_2O_3 to the zincate electrolyte, stirring overnight, and then filtering the electrolyte through a fine glass frit. The deposition studies were done on 1 × 1 cm "flag type" silver electrodes. The cell and the experimental procedures were identical with those described elsewhere [7]. In the potential-step measurements, a zinc reference electrode was used. This was in a separate compartment containing pure zincate electrolyte. The compartment was connected to the cell *via* a salt bridge consisting of a zincate-saturated cotton thread inside a thin PTFE tube (length: 20 cm). This procedure avoided contamination of the reference electrode by the bismuth. The electrolyte in the reference electrode compartment was de-aerated and provisions were made to prevent oxygen ingress to the reference electrode.

Results

Bi_2O_3 in pasted zinc electrodes

Chronopotentiometry

The results of the chronopotentiometry experiments in cells with 2 and 10 wt.% additions of Bi_2O_3 are given in Fig. 1. The results for an electrode with no additive are shown for comparison. The theoretical transition times for 2 wt.% Bi_2O_3 and 10 wt.% Bi_2O_3 are 20.4 and 102.0 min, respectively. The observed transitions therefore show that the Bi_2O_3 additive is essentially quantitatively reduced to bismuth prior to zinc deposition. This was confirmed by potentiostatic experiments. The zinc electrode potential was swept at 1 mV s^{-1} from −0.2 to −1.3 V and held there for 2 h. After the zinc oxide was dissolved, the grey bismuth metal remained.

Cyclic voltammetry

Figure 2 shows a set of cyclic voltammograms over various potential ranges for a 10 wt.% addition of Bi_2O_3. Initial sweeps between 0 and −0.6 V

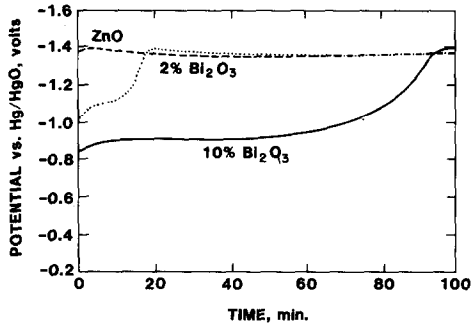

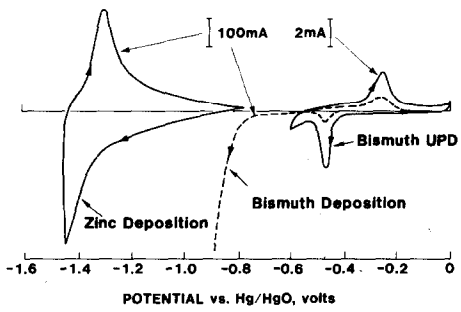

Fig. 1. Chronopotentiometry on pasted zinc oxide electrodes with 2 and 10 wt.% additions of Bi_2O_3; electrode area 38.7 cm^2; charge current 3.87 mA cm^{-2}. Results in absence of additive shown for comparison.

Fig. 2. Cyclic voltammograms for electrode with 10 wt.% Bi_2O_3; electrode area 38.7 cm^2; sweep rate 50 mV s^{-1}; anodic current positive; phenomena related to various cathodic processes are indicated on the Figure.

showed a cathodic peak at −0.48 V and an anodic peak at −0.25 V. We have attributed these peaks to underpotential deposition of bismuth on the silver current collector. On extending the negative limit of the potential to −0.85 V, there was a large increase in the cathodic current at −0.75 V. This corresponded to the onset of reduction of Bi_2O_3 to bismuth. The grey color of the bismuth metal could be seen through the cell wall. The electrode was held at −0.85 V for 2 h, and a final cyclic voltammogram was run over the potential range −0.8 to −1.45 V. The deposition and dissolution pattern for zinc could be plainly seen.

Electrode polarizability

The results of the electrode polarizability measurements were essentially identical with those found for an electrode without an additive [4].

Scanning electron microscopy

Figure 3 is a scanning electron micrograph of a charged electrode with Bi_2O_3 additive. The bismuth was in the form of a needle-like deposit that is distributed throughout the zinc electrode.

Electrodeposition of zinc on bismuth

Cyclic voltammetry

Figure 4 shows a typical cyclic voltammogram for a bismuth electrode in zincate electrolyte. No features that could be attributed to the underpotential deposition of zinc or to the formation of an alloy were observed. In the deposition region, the cyclic voltammogram displayed a nucleation loop [8].

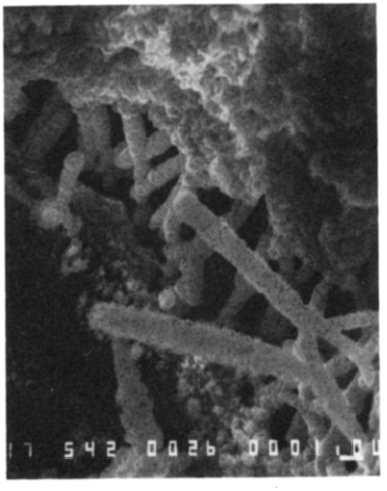

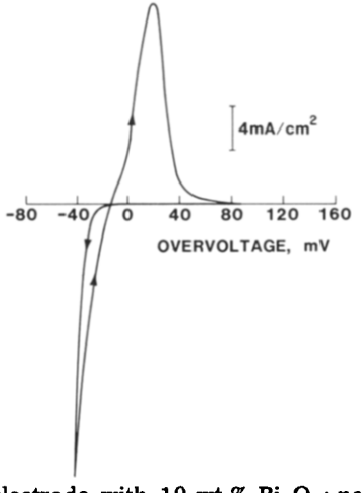

Fig. 3. Scanning electron micrograph of electrode with 10 wt.% Bi_2O_3; needle-like deposits of bismuth metal can be seen.

Fig. 4. Cyclic voltammogram for bismuth single crystal in 8.4M KOH + 0.74M ZnO; sweep rate 50 mV s^{-1}; anodic current positive.

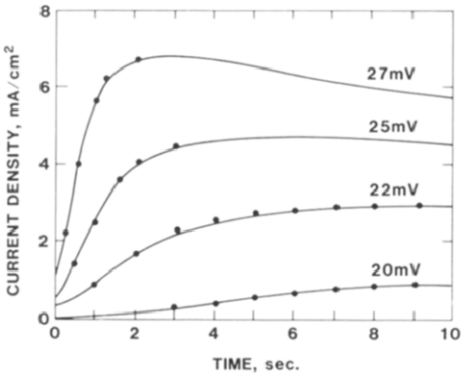

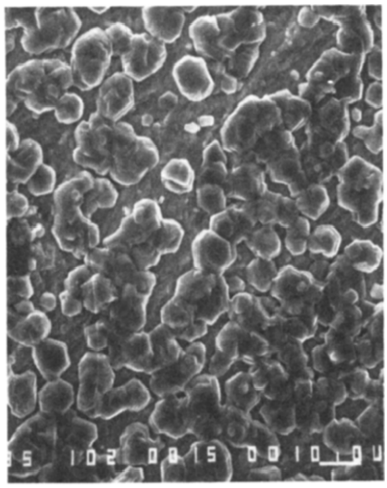

Fig. 5. Current transients (solid lines) for zinc deposition on single-crystal bismuth in 8.4M KOH + 0.74M ZnO; overvoltages indicated. Calculated values (●) are also shown.

Fig. 6. Scanning electron micrograph of zinc deposit on single-crystal bismuth. Deposition from an 8.4M KOH + 0.74M ZnO at 15 mA cm^{-2}; deposit of 5 C cm^{-2}.

Potential-step studies

Figure 5 shows the results of the potential-step studies. Below an overvoltage of 20 mV, no deposition was observed. Above 27 mV, the current transients displayed a maximum and the current decreased to a steady-state level.

Scanning electron microscopy and X-ray studies

Figure 6 is a scanning electron micrograph of a zinc deposit on bismuth. The deposit appears to consist of equal sized nuclei with an hexagonal morphology. Some of the nuclei have coalesced together. The X-ray diffraction results indicated that the deposit was oriented parallel to the basal plane.

Zinc deposition on silver

Cyclic voltammetry

Figure 7 shows a set of cyclic voltammograms in pure zincate (curve (a)) and in bismuth oxide-saturated zincate (curve (b)) electrolytes. In the case of curve (a), the patterns for underpotential deposition of zinc at about −1.25 V and alloy formation at about −1.3 V can be seen. These are similar to those reported by Adzic *et al.* [7]. In the case of curve (b), the anodic peak at −0.41 V first appeared on extending the cathodic limit to −0.75 V. This peak increased as the potential was extended in 100 mV increments to −1.3 V. The peak at −0.41 V has been attributed to stripping of bismuth metal. Formation of bismuth oxide would yield a reduction peak on the cathodic sweep. The results are consistent with bismuth deposition from soluble species under diffusion control. Bismuth deposition completely

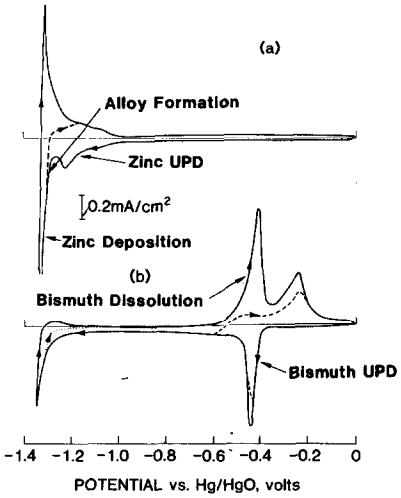

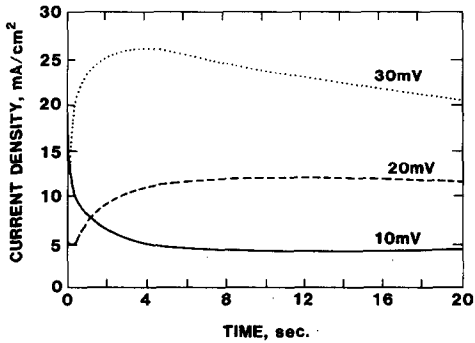

Fig. 7. Cyclic voltammograms for 1 x 1 cm silver "flag" electrodes: (a) 8.4M KOH + 0.74M ZnO; (b) same electrolyte saturated with Bi_2O_3.

Fig. 8. Current transients for zinc deposition on 1 x 1 cm silver flag electrodes in 8.4M KOH + 0.74M ZnO saturated with Bi_2O_3. Overvoltages indicated.

inhibits underpotential deposition of zinc on the silver and prevents alloy formation. In the absence of bismuth, there is a very large anodic stripping peak for zinc at −1.31 V when the negative limit is extended to −1.36 V (curve (a)). In the presence of bismuth, the corresponding anodic peak is very small, and the cathodic processes at potentials more negative than −1.2 V must be hydrogen evolution.

Potential-step studies

Figure 8 shows the results of the potential-step studies. Zinc deposition was observed at zinc overvoltages as low as 10 mV. This was true both for freshly prepared silver electrodes and for electrodes that had been cycled into the zinc-deposition region.

Discussion

Electrodeposition of zinc on bismuth

The potential-step results in Fig. 5 show rising current transients with an initial non-zero current that increases with potential. This initial current must be due to hydrogen evolution since no layer-type growth of zinc was observed. Hydrogen evolution is also consistent with the cyclic voltammetry results in Fig. 7(b). The initial part of the transient could be fitted to a simple electrocrystallization model that assumes instantaneous nucleation of zinc and growth of the nuclei under kinetic control [9 - 11]. The total current (i) can be expressed as

$$i = i_H + zFk_1\left[1 - \exp\left(\frac{-\pi M^2 k_2^2 N_o}{\rho^2}\right)\right]$$

where i_H is the current due to hydrogen evolution; k_1 and k_2 are the respective rates (mol cm^{-2} s^{-1}) of crystal growth of the nuclei in the directions perpendicular and parallel to the substrate; M is the molecular weight of zinc (65.38 g mol^{-1}); ρ is the zinc density (7.14 g cm^{-3}); N_o is the instantaneous nucleation rate; and t is the elapsed time from application of the potential step. Theoretical fits of i, calculated according to the above equation, are excellent. The values of zFk_1 and $k_2^2 N_o$ for various overvoltages are given in Table 2. The maxima and the decay in current at higher potentials can be analyzed in a manner described by Abyaneh *et al.* [11]. However, for the purposes of this discussion it suffices to say that the nucleation overvoltage on bismuth is about 20 mV, and that deposition proceeds *via* nucleation and growth of three dimensional centers that are oriented parallel to the basal plane.

TABLE 2

Values of i_H, zFk_1 and $k_2^2 N_o$ for zinc deposition on bismuth

Overvoltage (mV)	i_H (mA cm^{-2})	zFk_1 (mA cm^{-2})	$k_2^2 N_o$ (mol^2 cm^{-4} s^{-3})
20	0.08	0.71	1.5×10^{-4}
22	0.33	2.46	6.74×10^{-4}
25	0.70	3.71	2.27×10^{-3}
27	1.0	5.80	5.98×10^{-3}

Function of bismuth in the zinc electrode

Several effects are observed in the formation cycle when Bi_2O_3 is added to pasted zinc electrodes with silver current collectors. These are: (a) underpotential deposition of bismuth on the current collector (Fig. 2); (b) quantitative reduction of the additive to bismuth prior to zinc deposition (Fig. 1); (c) the formation of a needle-like matrix of bismuth in the zinc oxide paste (Fig. 3).

In pure zincate solutions, the deposition of zinc on silver involves underpotential deposition, alloy formation [7], and zinc deposition with negligible nucleation overvoltage (Figs. 7(a) and 8). Dissolved Bi_2O_3 in the zincate solution inhibits underpotential deposition, prevents alloy formation, and increases the nucleation overvoltage (Fig. 7). The effects are consistent with the formation of a bismuth coating on the silver. On bismuth, zinc deposition proceeds *via* a nucleation and growth process involving a critical nucleation overvoltage (Figs. 3 - 6).

Since the reversible potential for bismuth deposition is about 0.6 V more positive than zinc, no dissolution of the bismuth will occur prior to cell

failure at the end of life. The beneficial effect of bismuth cannot be due to a co-deposition effect. The other possibility is a substrate effect or an improvement in electrode conductivity in the presence of the bismuth matrix. One possible substrate effect is the inhibition of zinc deposition on the current collector and the promotion of a more even zinc distribution on the current collector and on the bismuth matrix. Without such inhibition, zinc deposits on silver with negligible overvoltage and is governed by the primary current distribution. The substrate can also affect zinc morphology [12, 13]. The deposit on bismuth is oriented parallel to the basal plane and such deposits tend to be active [12]. Active deposits mitigate the problem of zinc electrode densification. Several other oxide additives change the current distribution on zinc electrodes [4, 14]. Bismuth oxide does not [14]. The beneficial effect of bismuth is most likely, then, due to inhibition of the initial zinc deposition processes on the silver current collector, the maintenance of an active deposit, and the provision of a conductive matrix in the electrode during cycling.

In the case of oxide additives, quantitative reduction of HgO, Tl_2O_3 [4], and Bi_2O_3 has been observed prior to zinc deposition. At present, there is no obvious conduction mechanism for the current to get to the dispersed oxide particles in the paste.

References

1 T. Takamura, T. Shirogami, Y. Sato, K. Murata and H. Niki, *Brit. Pat. 1,44,695*, August 4, 1976.
2 M. Kanda, T. Shirogami, H. Niki, M. Ueno, K. Murata, Y. Sato and T. Takamura, Ext. Abstr. No. 94, *Electrochem. Soc., Proc. Vol. 80-2*, 1980 p. 256.
3 C. Biegler, R. L. Deutscher, S. Fletcher, S. Hua and R. Woods, *J. Electrochem. Soc., 130* (1983) 2303.
4 J. McBreen and E. Gannon, *Electrochim. Acta, 26* (1981) 1439.
5 W. J. McG. Tegart, *The Electrolytic and Chemical Polishing of Metals*, Pergamon Press, New York, 1959, p. 59.
6 J. McBreen and E. Gannon, *J. Electrochem. Soc., 130* (1983) 1667.
7 G. Adzic, J. McBreen and M. G. Chu, *J. Electrochem. Soc., 128* (1981) 1691.
8 A. R. Despic, in R. Weil and R. G. Barradas (eds.), *Proc. Symp. Electrocrystallization*, Electrochem. Soc., Pennington, NJ, 1981, p. 101.
9 M. Y. Abyaneh, M. Fleischmann and M. Labram, in R Weill and R. G. Barradas (eds.), *Proc. Symp. Electrocrystallization*, Electrochem. Soc., Pennington, NJ, 1981, p. 1.
10 M. Y. Abyaneh and M. Fleischmann, *Electrochim. Acta, 27* (1982) 1513.
11 M. Y. Abyaneh, J. Hendrikx, W. Visscher and E. Barendrecht, *J. Electrochem. Soc., 129* (1982) 2654.
12 M. G. Chu, J. McBreen and G. Adzic, *J. Electrochem. Soc., 128* (1981) 2281.
13 J. McBreen, M. G. Chu and G. Adzic, *J. Electrochem. Soc., 128* (1981) 2287.
14 J. McBreen and E. Gannon, *J. Electrochem. Soc., 130* (1983) 1980.